



Application of biochar and polyacrylamide to revitalize coastal saline soil quality to improve rice growth

Alimu Abulaiti^{1,2} · Dongli She^{1,2} · Zhipeng Liu³ · Xiaoqin Sun^{1,2} · Hongde Wang^{1,2}

Received: 25 May 2022 / Accepted: 4 October 2022 / Published online: 11 October 2022
© The Author(s), under exclusive licence to Springer-Verlag GmbH Germany, part of Springer Nature 2022

Abstract

Poor soil quality is affected by salinity, which limits land productivity and sustainable agricultural development in coastal China. Hence, it is essential to choose suitable and efficient approaches to revitalize coastal saline soil quality and improve agricultural productivity. Biochar and polyacrylamide (PAM) have been widely applied as soil amendments to enhance soil structure, but the interactive effects of biochar and PAM on rice growth are unclear. The experiment described in this study was conducted over five consecutive growing seasons (from 2016 to 2020) with biochar (at 0, 32, and 79 t/hm²) and PAM (at 0, 0.6, and 1.6 t/hm²) applications to study the effects of amendments on soil properties, rice photosynthesis, and rice yield in coastal saline land. The soil property results showed that wheat straw biochar and PAM lowered soil total salt and bulk density, but increased the soil organic matter (SOM), mean weight diameter of water-stable aggregates (MWD), and macroaggregate (> 0.25 mm) content. The application of either biochar or PAM increased the rice net photosynthetic rate, transpiration rate, and stomatal conductance. The combined application of 32 t/hm² biochar + 0.6 t/hm² PAM increased the net photosynthetic rate by 26.0% and the transpiration rate by 24.8% relative to the control. The application of 32 t/hm² biochar and 1.6 t/hm² PAM significantly increased the rice grain yield. The path analysis model showed that spikelets per panicle and canopy gross photosynthesis had strong and significant positive effects on grain yield, whereas soil total salt had a negative effect on grain yield. The combined application of 32 t/hm² biochar + 0.6 t/hm² PAM was identified as the most effective for rice growth. Biochar and PAM amendments at an optimal level may enhance soil properties by reducing salinity. These findings indicate that biochar and PAM have the potential to remediate coastal saline soil quality and the environment, which would simultaneously increase the sustainable use of coastal land resources and food production to preserve the ecological environment.

Keywords Saline soil · Biochar · Polyacrylamide · Soil physicochemical properties · Photosynthesis · Grain yield

Abbreviations

PAM	Polyacrylamide (t/hm ²)
MWD	Mean weight diameter of water-stable aggregates (mm)
CEC	Cation exchange capacity (cmol/kg)
TN	Total nitrogen (g/kg)
BD	Bulk density (g/cm ³)
Stage I	Tillering stage
Stage III	Heading-flowering stage
CGP	Canopy gross photosynthesis (mol.m ⁻²)
TGW	1000-Grain weight (g)
TS	Total salt (g/kg)
B1	0 T/hm ² biochar
B3	79 T/hm ² biochar
P2	0.6 T/hm ² PAM
SOM	Soil organic matter (g/kg)
OC	Organic carbon (g/kg)

Responsible Editor: Zhihong Xu

Zhipeng Liu is co-first author.

✉ Dongli She
shedongli@hhu.edu.cn

¹ College of Agricultural Science and Engineering, Hohai University, Nanjing 211100, China

² Jiangsu Province Engineering Research Center for Agricultural Soil-Water Efficient Utilization, Carbon Sequestration and Emission Reduction, Nanjing 211100, China

³ College of Resources and Environmental Sciences, Nanjing Agricultural University, Nanjing 210095, China

EC	Electrical conductivity (dS/m)
TP	Total porosity (%)
Stage II	Jointing-booting stage
Stage IV	Milky and yellow ripening stage
SSR	Seed setting rate (%)
SPP	Spikelets per panicle
Mas _{0.25}	Macroaggregates (>0.25 mm (%))
B2	32 T/hm ² biochar
P1	0 T/hm ² PAM
P3	1.6 T/hm ² PAM

Introduction

In recent years, under the multiple pressures of urbanization, population growth, and uncontrollable factors, such as climate change and the COVID-19 pandemic (Tatum 2021), the area of arable land available per capita has gradually decreased, the conflicts between human activities and land availability continue to intensify, and sustainable food production is hindered. Coastal reclamation areas are therefore becoming increasingly valuable as grain production bases (Xu et al. 2017), and scientifically revitalizing coastal saline soil has a critical role in remedying the shortage of arable land resources, ensuring national food security, and promoting sustainable agricultural development. However, soil salinization is a serious problem that can cause soil degradation, which limits plant growth and production in coastal reclamation regions (Ding and Yu 2014). The combined effects of sea tides, underground seawater intrusion, and human activities lead to soil degradation, resulting in poor soil structure, severe soil salinization, soil organic matter (SOM) deficiencies, low vegetation coverage, and serious deterioration of soil physicochemical properties, thereby limiting soil productivity (Yu et al. 2019; Sun et al. 2021). Hence, it is essential to revitalize the condition of saline soils to simultaneously improve land use efficiency and food production to preserve the ecological environment in coastal reclamation areas (Yang 2008). There are many ways to revitalize saline soils. Among them, soil amendments can significantly lower soil salinity, improve soil quality, and offer a suitable environment for corn growth (Zhao et al. 2020). In recent years, biochar and polyacrylamide (PAM) have been widely applied as soil amendments to enhance soil quality and environments (O'Laughlin and McElligott 2009; Fei et al. 2019).

Owing to the large surface area, high porosity, and strong ion absorption and exchange capacity of biochar, many studies have reported that biochar can reduce greenhouse gas emissions by fixing carbon, improve nutrient utilization and fertilizer availability, and thereby increase crop growth and yields (Tejada and Gonzalez 2007; Sohi et al. 2010; Xu et al. 2015; Ali et al. 2017). Cui et al. (2022) found that

the application of biochar (0, 20, 40, and 60 t/hm² wheat straw biochar) increased coastal saline soil pH, total soluble salt, and SOM by 0.2–3.1%, 12.6–139.6%, and 11.7–54.6%, respectively, compared with the control in a 3-year field experiment. In addition, biochar has been reported to reduce soil bulk density, which plays a significant role in improving soil micro- and mesoscale structure development, thereby increasing the number of macroaggregates in soil (Ajayi et al. 2016; Zhou et al. 2018). However, some previous studies found that biochar had no or even negative effects on soil physicochemical properties. Zhao et al. (2020) found that corn straw biochar significantly decreased soda saline-alkali soil pH in field experiments. Hardie et al. (2014) did not find any evidence that biochar application affected soil physical properties such as soil porosity by improving aggregate stability. The addition of 30 t/hm² biochar to weakly alkaline soil improved the corn photosynthetic rate by 16.5% and doubled the transpiration rate relative to the control in the Hetao irrigation district of Northwest China (Feng et al. 2021). Gaskin et al. (2010) also found that the application of 11 Mg/hm² peanut hull biochar with nitrogen fertilizer increased the grain yield of corn, whereas the application of 22 Mg/hm² peanut hull biochar with nitrogen fertilizer decreased the grain yield compared with the control. Hence, such discrepancies suggest that the effects of biochar on coastal saline soil physicochemical properties and crop yield are unclear.

PAM has strong water absorption and cohesion capacities, which allow it to help maintain a good soil structure (Lentz 2003; Tang and She 2018). PAM can effectively maintain soil aggregates and promote the formation of new aggregates (Nadler et al. 1996). These characteristics are beneficial to ameliorating soil structure and improving soil permeability (Yu et al. 2010). Moreover, PAM directly or indirectly affects the migration of soil nutrients, improves soil fertility retention, improves soil conditions, offers a suitable environment for plant growth, and increases crop yields (Han et al. 2010). In addition, Wang et al. (2016a, b) showed that the application of PAM to improve soil structure did not have significant effects on rice photosynthesis or fluorescence characteristics. Previous studies on PAM have focused mainly on its impacts on saline-sodic soil infiltration and erosion (Lentz 2003; Tang and She 2018). However, there have been few reports on the impact of PAM on revitalizing coastal saline soil quality, crop photosynthesis, and yield. An understanding of the effects of PAM on coastal saline soil physicochemical properties and crop production is also needed.

In this study, our objectives were to (a) investigate the interactive effects of biochar and PAM on saline soil properties and the photosynthetic traits and production of rice grown in a coastal reclamation area; (b) analyze the correlations among soil properties, photosynthesis, yield

components, and grain yield; and (c) characterize the contributions of soil properties, photosynthesis, and yield components to grain yield.

Materials and methods

Site description

The saline soils in our experiment were sampled in May 2015 from the Dongling coastal reclamation region in Rudong County, Jiangsu Province, China (120°42′–121°22′E and 32°12′–32°36′N), as shown in Fig. S1. The average elevation of the coastal reclamation region, which is located next to the Yellow Sea, is between 3.5 and 4.5 m. The soil in the coastal reclamation region is dominated by silty loam. The storage and transport of water in the soil are severely restricted due to the high content of sodium salt in the soil and the poor soil structure. The upper 100 cm soil layer of three sample plots with a length of 4 m and a width of 4 m in Rudong County was randomly selected. The soil samples were mixed thoroughly and brought back to the laboratory for experiments without external interference. During the rice planting seasons (June to November), the temperature in the greenhouse was adjusted to 28 ± 2 °C. The annual mean precipitation is 1044.7 mm, and the annual mean surface water evaporation is 1367.9 mm. More details about the methods used to measure basic soil physico-chemical properties are shown in our previous study (Fei et al. 2019). The basic soil physico-chemical properties are shown in Table 1.

Experimental design

The study was conducted for five consecutive seasons in a completely randomized design from 2016 to 2020. The test pit cultivation experiment was carried out in a greenhouse that provided shelter from the rain. The test pits had an upper diameter of 840 mm and a height of 850 mm, each of

approximately 300 L (Fig. 1). The test pit was buried below the ground, and the inverted layer was set at the bottom of the test pit with a thickness of 50 mm, and sand, gravel with different particle sizes were placed in the inverted layer. In order to achieve the purpose of smooth groundwater flow and no loss of fine particles in the soil, the grading and hierarchical arrangement of the inverted layer were correctly done in this pit experiment. The upper part of the inverted layer was filled with air-dried and sieved soil (bulk density of 1.38 g/cm^3) with a thickness of 500 mm, and the soil was compacted and flattened. Biochar (at 0, 32, and 79 t/hm², denoted by B1, B3, and B3, respectively) and PAM (at 0, 0.6, and 1.6 t/hm², denoted by P1, P2, and P3, respectively) were uniformly mixed with the surface soils (0–20 cm) of the test pits on June 1, 2016, and 4 repetitions of each application rate were established, for a total of $3 \times 3 \times 4 = 36$ test pits (Table S1). A drain pipe was installed in the test pit to extract groundwater. Every test pit was subjected to the same management measures (e.g., amount of irrigation and fertilizer application) to reduce interference from other external factors and human factors in this experiment. Considering the timeliness of the effects of amendment application, the amendments were repurchased and added again on June 1, 2020. The repurchased biochar and PAM were evenly mixed with the 0–20 cm soil layer of each treatment. The amounts and characteristics of the amendments reapplied in 2020 were consistent with those in the experiments in 2016.

Biochar and PAM characterization

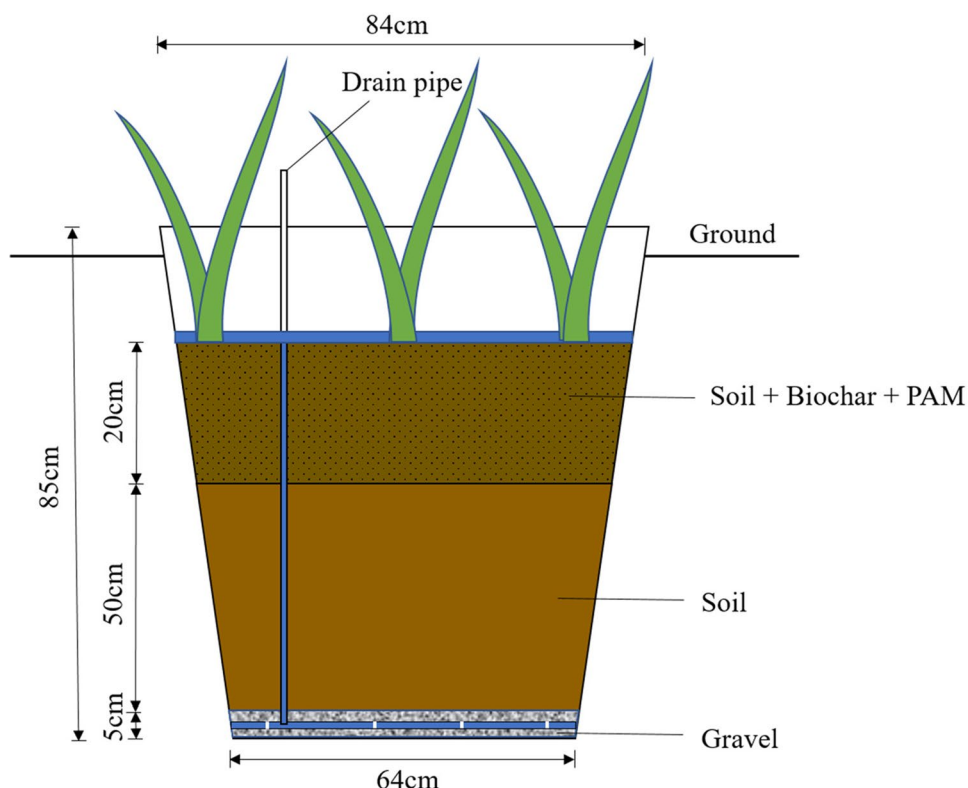
The biochar applied in this research was produced by the pyrolysis of wheat straw at 350–550 °C, and the conversion rate of wheat straw into biochar was 30%. More detailed methods regarding the determination of the physicochemical properties of the biochar can be found in our previous research (Fei et al. 2019). The relative molecular weight of PAM was measured by viscometry. The physicochemical properties of the biochar and PAM are presented in Table 1.

Table 1 Basic properties of the soil, biochar, and PAM

Soil		Texture		OC (g/kg)	TN (g/kg)	BD (g/cm ³)	pH	EC (dS/m)	CEC (cmol/kg)	
Size composition (%)		Silt	Clay							
Sand		62.75	4.88	Silt loam	3.81	0.41	1.38	8.0	4.0	4.99
Biochar										
Ca (g/kg)	Particle density (g/cm ³)	TP (%)	Cl (g/kg)	OC (g/kg)	TN (g/kg)	BD (g/cm ³)	pH	EC (dS/m)		
0.0016	1.83	62.5	1.44	467.2	5.9	0.69	9.9	1.0		
PAM										
Property	Molecular weight									
Anionic	12 million									

CEC cation exchange capacity, OC organic carbon, TN total nitrogen, EC electrical conductivity, BD bulk density, TP total porosity

Fig. 1 Conceptual diagram of the test pit cultivation experiment



Agricultural applications

Planting crop is one of the important ways to revitalize saline soil in a coastal reclamation region. Therefore, before planting rice, the refilled soil in the test pit was irrigated and incubated for 6 months. A high-yielding rice variety, Wu Yun Jing 23, was used each year (from 2016 to 2020) in our experiment. The rice planting density was 162,000 hills/hm², and there were 2 root seedlings/hill. Two days before transplanting the rice seedlings, the saline soils in the test pits were plowed and harrowed (to a soil depth of 20 cm from the surface) by hand. The standard nitrogen application rate for the paddy rice fields was 300 kg/hm², and the ratio of basal fertilizer to top dressing fertilizer was 6:4. Compound fertilizer was used as the basal fertilizer, and 50 g was added to the soil surface per test pit. Five grams of topdressing fertilizer (urea, 46.4% nitrogen) was applied per test pit. Twenty-four hours before transplanting the rice seedlings, basal fertilizer was added to the saline soil, tillering fertilizer (urea) was added approximately 10 days after transplanting, and ear fertilizer (urea) was added before the booting stage. The fertilizers were mixed evenly in the upper saline soils (0–20 cm) before the rice seedlings were transplanted (Wang et al. 2017). After the rice seedlings were transplanted, each test pit (buried in the ground) and its surrounding environment were manually weeded every month to eliminate the influence of weeds on rice growth. All other recommended cultivation practices were applied

to maximize rice production. The irrigation volume of each measuring bucket was the same; the lower limit of irrigation water was 30 mm, and the upper limit of irrigation was 50 mm. The date and amount of irrigation were recorded each time. The groundwater drainage rate of each test pit was 5 mm/day. The dates for rice seed cultivation, transplanting, fertilization, and harvesting in this experiment are shown in Table 2.

Rice yield measurements

The rice was harvested manually and threshed using a hand-driven thresher each year (from 2016 to 2020). Rice grains were collected and dried at 105 °C for 1 h and then dried at 80 °C for 48 h to constant weight. Yield components such as the 1000-grain weight, spikelets per panicle, and seed-setting rate were obtained from 15 rice plants randomly selected from each test pit.

Soil measurements

For five consecutive seasons (from 2016 to 2020), 0–20 cm of topsoil was collected after the annual rice harvest to measure soil physical and chemical properties such as pH, total salt, SOM, bulk density, mean weight diameter (MWD), and macroaggregates. The soil pH was determined at a soil-to-water mass ratio of 1:5 using a pH meter. The content of soil cations (K⁺, Na⁺, Ca²⁺, Mg²⁺) was determined

Table 2 Dates for rice seed cultivation, transplanting, fertilization, harvesting, and photosynthesis measurements

Classification	Years				
	2016	2017	2018	2019	2020
Seed cultivation	June 5	May 30	June 1	June 5	June 5
Transplanting	June 29	June 23	June 25	June 29	July 1
Basal fertilizer (NPK compound fertilizer) application	June 30	June 24	June 26	June 30	July 2
Tillering fertilizer (urea) application	July 10	July 5	July 9	July 9	July 10
Ear fertilizer (urea) application	August 10	August 7	August 10	August 9	August 10
Harvest	October 25	October 26	October 26	October 25	October 27
Photosynthesis measurements	Stage I			July 12	July 15
	Stage II			August 6	August 10
	Stage III			September 2	September 5
	Stage IV			September 26	September 28

Stage I, tillering stage; stage II jointing-booting stage; stage III, heading-flowering stage; stage IV, milky and yellow ripening stage

by an inductively coupled plasma emission spectrometer (Optima 8000). The content of CO_3^{2-} and HCO_3^- ions in the soil was determined by the phenolphthalein and methyl orange double indicator neutralization method, and Cl^- and SO_4^{2-} in the soil were determined by the silver nitrate titration method and ethylenediaminetetraacetic acid (EDTA) titration method, respectively. The soil total salt content was expressed as the sum of soil cations and anions. The SOM was measured in an externally heated oil bath using the potassium dichromate wet combustion method (Schepetkin et al. 2003). The soil bulk density was determined by the drying method (Cueff et al. 2021). According to Wang et al. (2015), soil water-stable aggregates were characterized by MWD. More details about the methods used to measure the macroaggregate (> 0.25 mm) content are shown in our previous study (Fei et al. 2019).

Measurements of photosynthetic parameters

The photosynthetic parameters of rice were measured in the two seasons of 2019 and 2020. During the course of the experiment, the net photosynthetic rate, transpiration rate, and stomatal conductance of the top fully expanded rice leaves were measured in four growth stages (the tillering stage, jointing-booting stage, heading-flowering stage, and milky and yellow ripening stage, called stage I, stage II, stage III, and stage IV, respectively). The assessment dates for the photosynthetic parameters are shown in Table 2. A gas exchange analyzer (LI-6800, LI-COR, USA) was used to measure these photosynthetic parameters from 09:00 to 11:00 when the photosynthetically active radiation above the canopy was $1000 \sim 1100 \mu\text{mol}/\text{m}^2 \text{ s}$, and the temperature was $28 \pm 2 \text{ }^\circ\text{C}$. Rice leaves were randomly selected from five hills in each test pit, and the mean of the five rice leaves was used as the final fixed value. The daily dynamics of the net photosynthetic rate and transpiration

rate were determined from 08:00 to 18:00 on July 22, 2019, and July 29, 2020.

Estimation of daily cumulative photosynthesis and canopy gross photosynthesis

The daily cumulative photosynthesis was calculated according to the daily change in the observed net photosynthetic rate under biochar and PAM amendments.

$$\sum P_n = \frac{1}{2} \cdot \sum_{i=1}^{n-1} (P_{n(i)} + P_{n(i+1)}) \cdot H_i \quad (1)$$

where $\sum P_n$ is the daily cumulative photosynthesis of a single leaf, mmol/m^2 ; $P_{n(i)}$ and $P_{n(i+1)}$ are the net photosynthetic rates determined at the i -th and $(i+1)$ -th times, respectively, $\mu\text{mol}/(\text{m}^2 \text{ s})$; H_i is the time interval between the i -th and $(i+1)$ -th determinations; and n is the number of determinations.

According to Miao et al. (2013), the instantaneous net photosynthetic rate of a single leaf was used to calculate the corresponding daily cumulative photosynthesis. A regression analysis of the net photosynthetic rate at 10:00 from the observed daily changes in rice photosynthesis and the corresponding daily cumulative photosynthesis was performed, as shown in Fig. S2. The linear regression equation is as follows:

$$\sum P_n = 15.479P_n + 238.08 \quad (R^2 = 0.8745) \quad (2)$$

where P_n is the instantaneous net photosynthetic rate of a single leaf at 10:00 and $\sum P_n$ is the daily cumulative photosynthesis of a single leaf.

The cumulative photosynthesis in the canopy was estimated based on the principle of the big-leaf model (Pury and Farquhar 1997). The calculation formula is as follows:

$$P_c = P_n \times \text{LAI} \quad (3)$$

where P_c is the canopy net photosynthetic rate, P_n is the single-leaf net photosynthetic rate, and LAI is the canopy leaf area index.

The linear regression function in Eq. (2) was used to calculate the daily cumulative photosynthesis in rice leaves at the different growth stages with biochar and PAM. Then, the daily canopy cumulative photosynthesis was determined using the LAI observed at each growth stage (from stage I to stage IV). The rice LAI was determined at each growth stage using a METER plant canopy analyzer (AccuPAR-LP-80, USA), and the average value after three measurements of each test pit was regarded as the final LAI. Finally, the daily canopy cumulative photosynthesis values throughout the growth period were summed to obtain the canopy gross photosynthesis.

Statistical analysis

One-way analysis of variance (ANOVA) and multiple comparisons (least significant difference (LSD), significance level of $P=0.05$) were conducted using SPSS (version 22.0, IBM, USA) to statistically analyze the experimental data. Descriptive statistics for the data, including their standard deviations, normal distribution test results, and Pearson linear correlation coefficients, were calculated. Correlation

coefficients were divided into direct and indirect coefficients using path coefficient analysis (Guner et al. 2017). Path analysis is an extension of regression analysis and can be used to analyze the causal structure of data. Causal relationships were explained via the path diagram, from which the direct and indirect effects of soil properties, yield components, and photosynthesis on rice grain yield could be distinctly determined (Fig. 2).

Results

Soil physicochemical properties under biochar and PAM amendments

Table 3 shows the mean values of soil pH, total salt, SOM, bulk density, MWD, and macroaggregates (> 0.25 mm) for each biochar and PAM treatment in the five growing seasons (from 2016 to 2020). The pH was significantly increased in the 79 t/hm² biochar treatment compared with the 0 t/hm² and 32 t/hm² biochar treatments ($P < 0.001$), whereas the application of PAM and the interaction of biochar and PAM had no significant effect on soil pH. In addition, the soil pH differences between years were not significant (Table S2). The level of soil total salt was significantly lower under 32 t/hm² biochar treatment than under 0 t/hm² and 79 t/hm² biochar treatments. The lowest total salt occurred under the combined application of 32 t/hm² biochar and 0.6 t/hm²

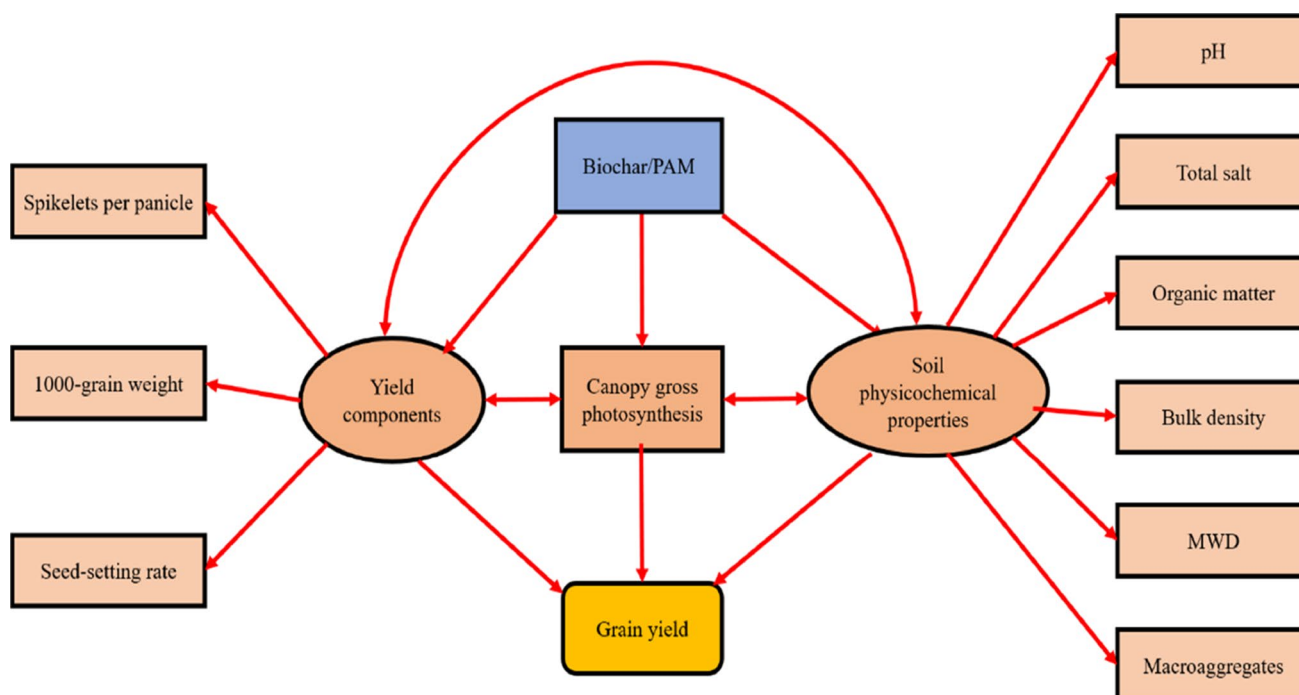


Fig. 2 A generalized conceptual framework of the path analysis model for the direct and indirect effects of influencing factor interactions on grain yield

Table 3 Effects of amendments on soil physicochemical properties in 2016–2020

Treatments		pH	Total salt (g/kg)	Organic matter (g/kg)	Bulk density (g/cm ³)	MWD (mm)	Macroaggregates (>0.25 mm (%))
Biochar (t/hm ²)	PAM (t/hm ²)						
0	0	7.90 (0.05) c	5.18 (0.93) b	5.89 (1.07) c	1.327 (0.071) a	0.322 (0.038) d	10.416 (1.438) d
	0.6	7.90 (0.05) c	5.27 (0.86) b	6.15 (1.04) c	1.303 (0.062) ab	0.382 (0.048) c	11.737 (1.994) cd
	1.6	7.91 (0.08) c	5.79 (1.01) ab	6.54 (1.06) c	1.300 (0.037) ab	0.400 (0.103) bc	13.932 (4.605) b
32	0	8.00 (0.07) b	4.76 (0.84) c	11.40 (3.47) b	1.327 (0.062) a	0.383 (0.074) c	15.266 (3.399) ab
	0.6	7.94 (0.10) c	4.18 (0.84) c	12.24 (3.75) b	1.294 (0.077) b	0.436 (0.052) ab	16.098 (1.531) a
	1.6	8.01 (0.08) b	4.42 (0.79) c	13.15 (4.09) b	1.287 (0.039) b	0.466 (0.082) a	17.560 (3.328) a
79	0	8.05 (0.06) ab	4.57 (0.74) c	19.03 (6.54) a	1.288 (0.053) b	0.416 (0.047) b	16.045 (2.157) a
	0.6	8.08 (0.03) a	5.94 (1.43) a	20.96 (7.59) a	1.271 (0.044) bc	0.442 (0.108) ab	16.815 (3.967) a
	1.6	8.05 (0.05) ab	5.42 (0.95) b	21.42 (7.54) a	1.253 (0.024) c	0.470 (0.088) a	17.752 (4.825) a
ANOVA							
Biochar		***	***	***	***	***	***
PAM		ns	**	ns	***	***	***
Biochar × PAM		ns	***	ns	ns	ns	ns

Different letters in the same column show that the difference among different treatments reached a significant level ($P < 0.05$). * ($P < 0.05$); ** ($P < 0.01$); *** ($P < 0.001$); ns ($P > 0.05$)

MWD mean weight diameter of water-stable aggregates

PAM, and the salinity decreased year by year (Table S3). Moreover, the interaction of biochar and PAM had a significant effect on soil total salt (Table 3). SOM was affected significantly by biochar application and increased as the biochar and PAM application rates increased. The soil bulk density was significantly lower under 79 t/hm² biochar addition than under 0 t/hm² and 32 t/hm² biochar additions, and the bulk density was reduced as the biochar and PAM addition rates increased. The soil MWD and macroaggregates (>0.25 mm) in the 1.6 t/hm² PAM treatment were significantly higher than those in the control (0 t/hm² PAM), while no significant differences in MWD occurred between 0.6 t/hm² and 1.6 t/hm² PAM treatments. The soil MWD and macroaggregates (>0.25 mm) in the 79 t/hm² biochar treatment were significantly larger than those in the control (0 t/hm² biochar), which indicated that the effects of biochar on the soil MWD and macroaggregates (>0.25 mm) were similar to the effect of biochar on SOM. After the application of biochar and PAM, SOM, MWD, and macroaggregate (>0.25 mm) content increased year by year, whereas the bulk density decreased year by year (Tables S4–S7).

Photosynthetic traits under biochar and PAM amendments

Biochar and PAM had significant effects on the rice leaf photosynthetic traits (Figs. 3 and 4). The rice leaf photosynthetic traits reached peak values in the B2 (32 t/hm² biochar) treatment. Compared to that in the control (0 t/hm² biochar), the

net photosynthetic rate under the B2 treatment from stage I to stage IV improved by average values of 11.29%, 2.03%, 14.4%, and 20.38%, respectively, whereas that under the B3 (79 t/hm² biochar) treatment at stage II decreased by an average of 11.96%. The effect of the B2 treatment on the transpiration rate was greater in 2020 than in 2019. Compared with that in the control, the stomatal conductance under the B2 treatment increased by 15.83%, 4.89%, 6.85%, and 22.4% on average during the four growth stages, while that under the B3 treatment decreased by 0.64%, 7.17%, 6.82%, and 9.96% on average. The photosynthetic traits increased with increasing PAM addition rate, and the increases in stage III and stage IV were especially obvious in 2020.

Figure 5 shows that the daily dynamics of the net photosynthetic rate showed a bimodal curve and that daily cumulative photosynthesis exhibited an S-shaped growth curve. Biochar improved daily dynamics of the leaf net photosynthetic rate of rice (Fig. 5). With the continuous accumulation of photosynthates, the differences in the daily cumulative photosynthesis among the treatments were obvious. The daily cumulative photosynthesis in the B2P1 (32 t/hm² biochar + 0 t/hm² PAM) treatment was the highest, followed by that in the B3P1 (79 t/hm² biochar + 0 t/hm² PAM) treatment. PAM (0.6, 1.6 t/hm²) increased the average daily net photosynthetic rate by 12.4% and 15.8%, respectively, and daily cumulative photosynthesis by 10.9% and 11.7%, respectively, compared with the control. The difference in daily cumulative photosynthesis between the B1P2 (0 t/hm² biochar + 0.6 t/hm² PAM) and

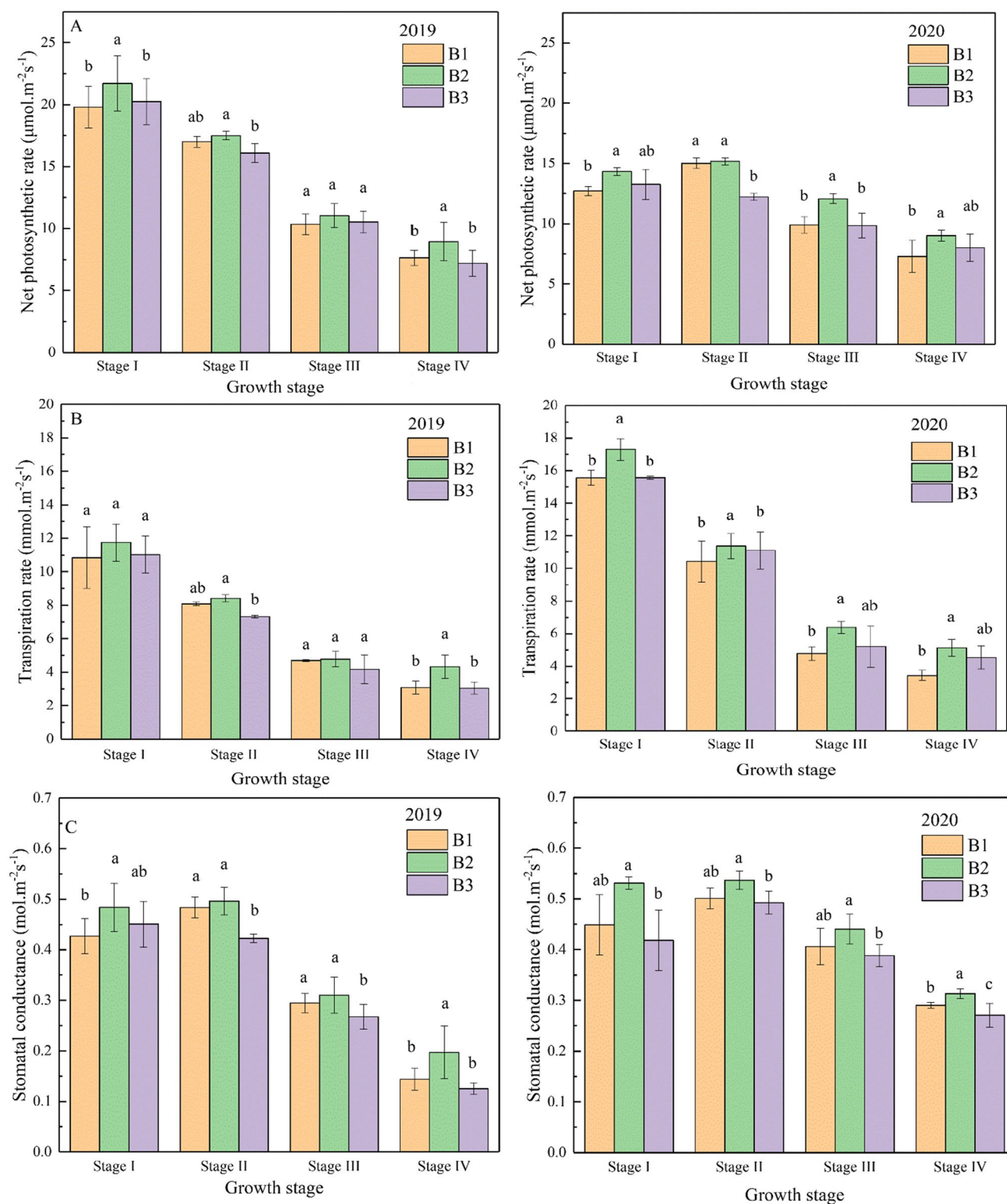


Fig. 3 Net photosynthetic rate (A), transpiration rate (B), and stomatal conductance (C) under biochar amendment treatments throughout the growth period. Stage I, tillering stage; stage II, jointing-booting stage; stage III, heading-flowering stage; stage IV, milky and yellow

ripening stage. B1, 0 t/hm² biochar; B2, 32 t/hm² biochar; B3, 79 t/hm² biochar. Different lowercase letters in the same column show that the difference between different biochar application amounts reached a significant level ($P < 0.05$)

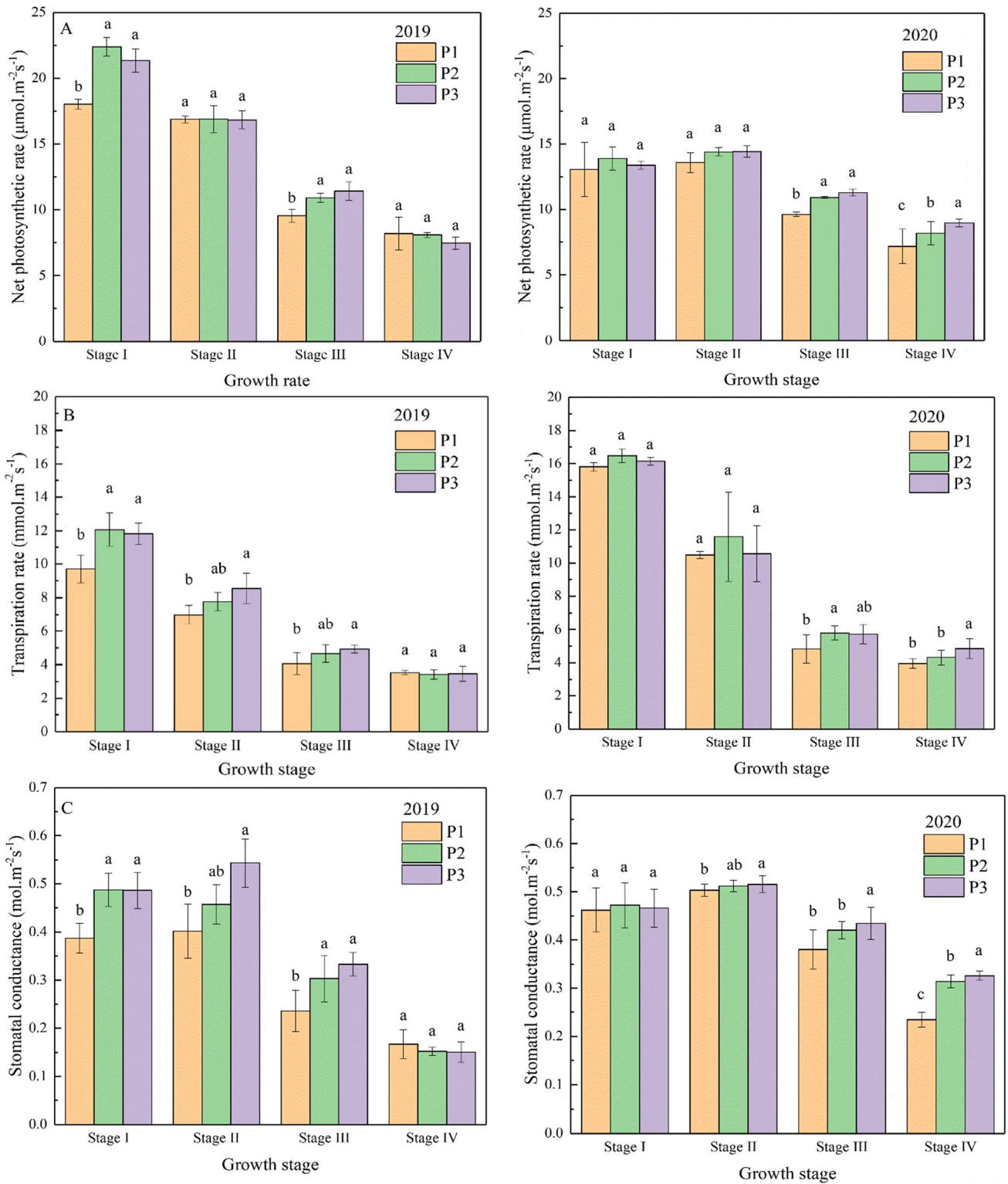


Fig. 4 Net photosynthetic rate (A), transpiration rate (B), and stomatal conductance (C) under PAM amendment treatments throughout the growth period. Stage I, tillering stage; stage II, jointing-booting stage; stage III, heading-flowering stage; stage IV, milky and yellow

ripening stage. P1, 0 t/hm² PAM; P2, 0.6 t/hm² PAM; P3, 1.6 t/hm² PAM. Different lowercase letters in the same column show that the difference between different PAM application amounts reached a significant level ($P < 0.05$)

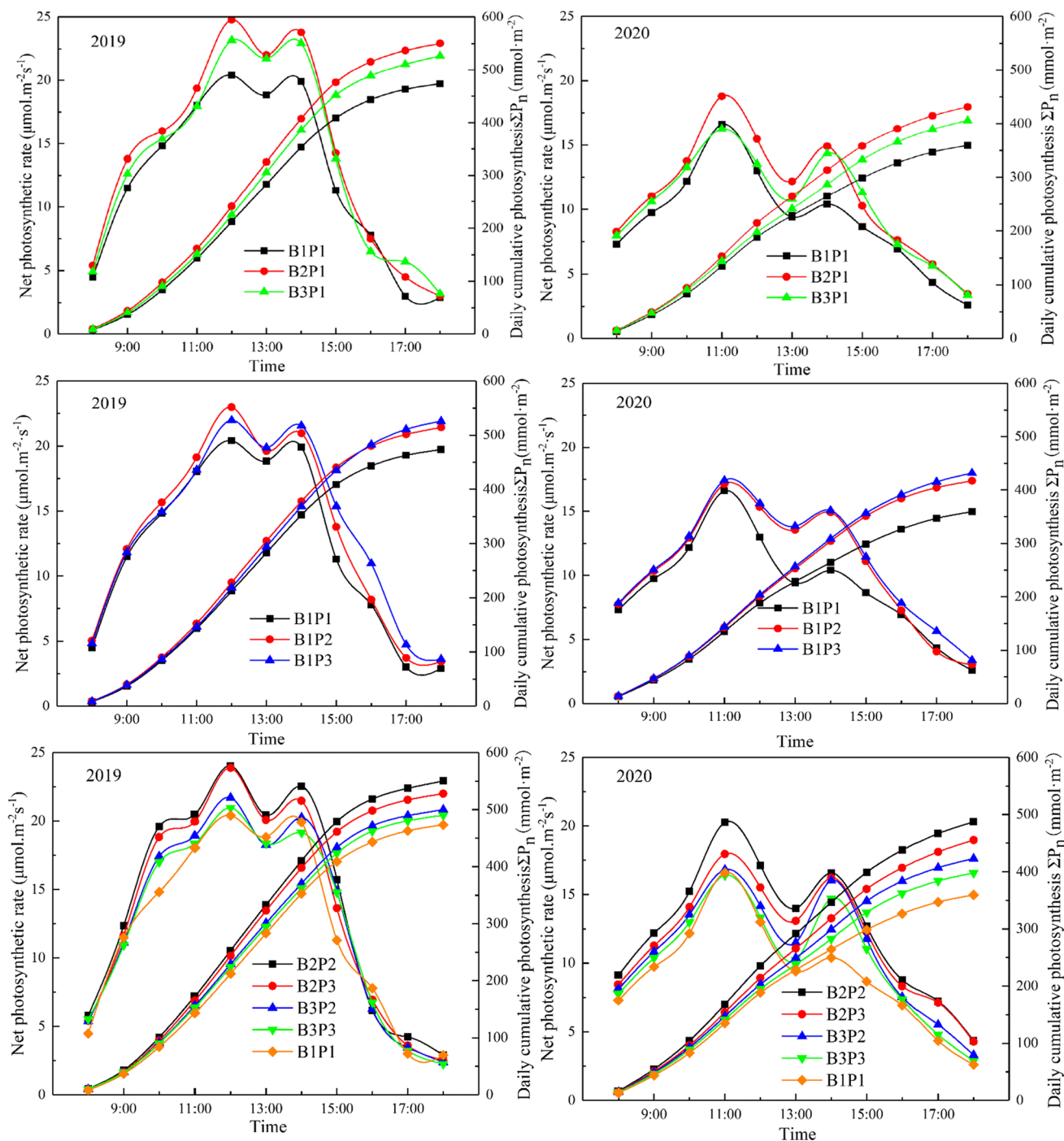


Fig. 5 Daily dynamics of the net photosynthetic rate under biochar and PAM treatments. B1, 0 t/hm² biochar; B2, 32 t/hm² biochar; B3, 79 t/hm² biochar; P1, 0 t/hm² PAM; P2, 0.6 t/hm² PAM; P3, 1.6 t/hm² PAM

B1P3 (0 t/hm² biochar + 1.6 t/hm² PAM) treatments was very small. The combined application of biochar and PAM improved the rice net photosynthetic rate, and the 32 t/hm² biochar + 0.6 t/hm² PAM combined treatment resulted in the highest daily cumulative photosynthesis of all combined treatments (Fig. 5).

The diurnal change curve of the rice transpiration rate was bimodal (Fig. 6). The overall treatment curves of biochar with PAM (0.6, 1.6 t/hm²) revealed an increase in the average daily dynamics of leaf transpiration rates by 6.0% and 10.8%, respectively (Fig. 6). The combination of biochar and PAM, especially the 32 t/hm² biochar + 0.6

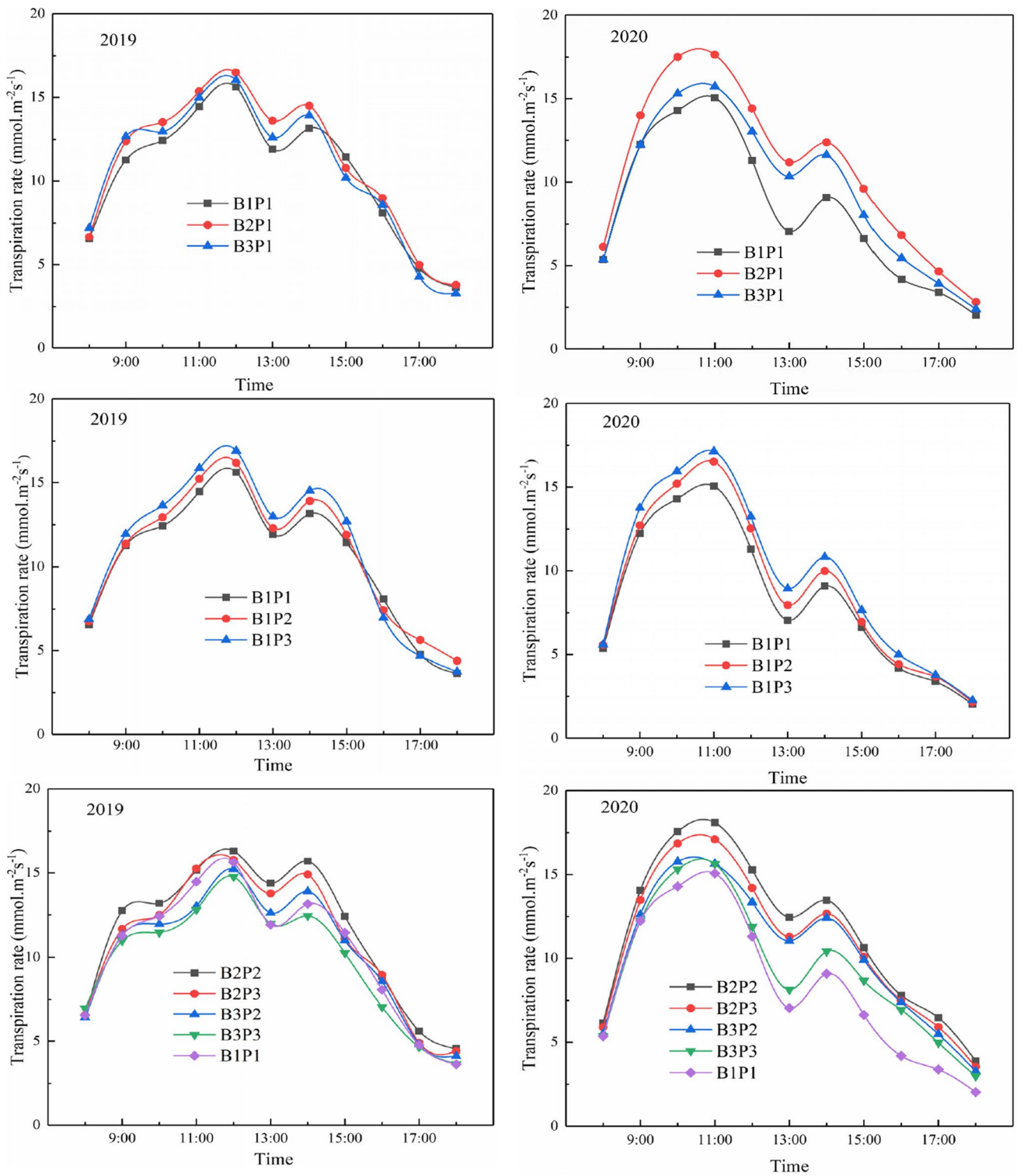


Fig. 6 Daily dynamics of the transpiration rate under biochar and PAM treatments. B1, 0 t/hm² biochar; B2, 32 t/hm² biochar; B3, 79 t/hm² biochar; P1, 0 t/hm² PAM; P2, 0.6 t/hm² PAM; P3, 1.6 t/hm² PAM

t/hm² PAM treatment, increased the average daily photosynthetic rate by 26% and the transpiration rate by 24.8% compared with those of the control. The change trends in

the net photosynthetic rate and transpiration rate in each treatment were basically the same: the first peak occurred from approximately 11:00 to 12:00, the values decreased to

a minimum by approximately 13:00 and then increased, and a second peak occurred at approximately 14:00.

Regression analysis of the net photosynthetic rate at 10:00 against the actual daily changes in rice photosynthesis and the corresponding daily cumulative photosynthesis was performed, as shown in Fig. S2. The R^2 value was 0.8745. The regression results showed that the linear relationship between the net photosynthetic rate at 10:00 and daily cumulative photosynthesis was acceptable. Table S8 lists the daily cumulative photosynthesis and canopy gross photosynthesis of rice under the biochar and PAM treatments in 2019 and 2020. Table S8 shows that canopy gross photosynthesis was the highest under the 32 t/hm² biochar + 0.6 t/hm² PAM combined treatment.

Impacts of biochar and PAM amendments on rice yield

The grain yield and yield components were significantly affected by biochar and PAM ($P < 0.05$) (Table 4). The grain yield did not show a positive linear increasing trend with increasing biochar and PAM application rates; rather, it showed a trend of first increasing and then decreasing. Under the same soil amendment treatment, the grain yield increased from 2016 to 2020 (Table S12), and the interaction of biochar and PAM had significant effects on rice yield components (spikelets per panicle, seed setting rate, and 1000-grain weight). Compared with that of the control (0 t/hm² biochar), the grain yield under 32 t/hm² biochar treatment increased by 11.0%, while that under 79 t/hm² biochar treatment decreased by 1.6%. The grain yield under 0.6

and 1.6 t/hm² PAM treatments increased by 16.5% and 3.2% compared with that of the control (0 t/hm² PAM), respectively. Moreover, the grain yield was the highest under 32 t/hm² biochar + 0.6 t/hm² PAM combined treatment compared to the control (0 t/hm² biochar + 0 t/hm² PAM) and reached 5842.1 kg/hm² to 7945.1 kg/hm².

Correlations among soil properties, canopy gross photosynthesis, yield components, and grain yield

Bivariate correlation analysis showed that grain yield was significantly and strongly positively ($P < 0.05$) correlated with yield components (spikelets per panicle, seed setting rate, and 1000-grain weight) and canopy gross photosynthesis. However, soil physicochemical properties (pH, total salt, SOM, and bulk density) had a small negative correlation with grain yield (Table S13).

Table 5 shows the direct and indirect effects of individual variables on the rice grain yield obtained by path analysis and the contribution of the determination coefficient. The direct effect coefficient of spikelets per panicle on grain yield was the highest, and the determination coefficient also showed that the number of spikelets per panicle was the most significant parameter with respect to grain yield. In addition, the direct effect coefficient of variables and the determination coefficients of variables on grain yield indicated that canopy gross photosynthesis played an important role in grain yield. Although soil total salt and SOM had positive direct effects on yield, the determination coefficients showed that they ultimately had negative effects on grain yield. The determination coefficients also demonstrated that the seed

Table 4 Effects of amendments on rice grain yield and yield components in 2016–2020

Treatments		1000-grain weight (g)	Spikelets per panicle	Seed-setting rate (%)	Grain yield (kg/hm ²)
Biochar (t/hm ²)	PAM (t/hm ²)				
0	0	24.9 (1.7) b	128.5 (1.4) de	84.7 (1.2) d	5842.1 (424.8) c
	0.6	25.5 (1.9) b	137.7 (3.7) c	87.0 (1.1) b	6918.0 (1050.0) b
	1.6	25.3 (1.6) b	134.8 (3.1) d	87.7 (0.4) b	6435.3 (650.7) b
32	0	25.1 (2.1) b	134.7 (4.1) d	86.7 (1.2) c	6689.4 (630.3) b
	0.6	26.5 (2.2) a	155.9 (7.5) a	89.1 (1.0) a	7945.1 (1260.0) a
	1.6	25.6 (1.9) b	135.8 (2.7) cd	88.2 (0.8) ab	6674.2 (626.2) b
79	0	25.2 (1.5) b	127.5 (7.1) e	86.6 (1.7) c	6044.6 (610.7) c
	0.6	24.9 (1.9) b	144.9 (2.5) b	87.3 (1.3) b	6785.9 (845.2) b
	1.6	24.8 (1.7) b	127.2 (10.2) e	87.0 (0.6) b	6064.5 (676.3) c
ANOVA					
Biochar		**	***	***	***
PAM		*	***	***	***
Biochar × PAM		*	***	***	ns

Different letters in the same column show that the difference among different treatments reached a significant level ($P < 0.05$). * ($P < 0.05$); ** ($P < 0.01$); *** ($P < 0.001$); ns ($P > 0.05$)

Table 5 Path analysis of the effects of canopy gross photosynthesis, yield components, and soil physicochemical properties on grain yield

Variables	Correlation coefficient	Direct path coefficient	Determination coefficient	Indirect path coefficient									
				Total	Via CGP	Via SSR	Via TGW	Via SPP	Via pH	Via TS	Via SOM	Via BD	Via MWD
CGP	0.876	0.464	0.598	0.412	0.434	0.036	-0.168	-0.062	-0.007	0.002	-0.067		
SSR	0.643	0.253	0.261	0.389	0.307	-0.018	-0.139	0.105	-0.022	0.026	-0.169		
TGW	0.575	0.178	0.173	0.396	0.194	0.112	-0.120	-0.150	0.007	-0.011	0.045		
SPP	0.899	0.540	0.678	0.358	0.373	0.144	-0.131	-0.009	-0.020	0.004	-0.076		
pH	-0.306	-0.160	0.072	-0.146	-0.029	0.009	-0.014	0.239	-0.014	0.023	-0.149		
TS	-0.395	0.276	-0.294	-0.670	-0.255	0.008	-0.096	0.000	-0.011	0.171			
OM	-0.187	0.318	-0.219	-0.504	-0.015	-0.120	-0.083	-0.018	0.030	-0.207			
BD	-0.371	0.044	-0.035	-0.416	-0.242	0.049	-0.130	-0.031	-0.031	0.111			
MWD	0.046	0.047	0.002	0.000	0.050	-0.079	0.202	-0.029	-0.029	-0.199			
Mas _{0.25}	0.160	-0.255	-0.148	0.417	0.161	-0.094	0.258	-0.019	0.037				

CGP canopy gross photosynthesis (mol m⁻²), SSR seed setting rate (%), TGW 1000-grain weight (g), SPP spikelets per panicle, TS total salt (g/kg), SOM soil organic matter, BD bulk density (g/cm³), MWD mean weight diameter of water-stable aggregates (> 0.25 mm (%))

setting rate and 1000-grain weight had positive effects on grain yield, whereas the soil macroaggregate (> 0.25 mm) content had a small negative effect on grain yield. Moreover, the direct negative effect of pH on grain yield was small, and the final contribution of pH to grain yield was not significant.

Discussion

Soil properties and photosynthetic traits under biochar and PAM amendments

Previous studies found that biochar amendments had significant effects on saline soil characteristics. The soil pH was improved from 8.13 to 8.24 using wheat straw biochar in saline soil (Liu et al. 2019). Cui et al. (2022) also found that the application of biochar (0, 20, 40, and 60 t/hm² wheat straw biochar) increased coastal saline soil pH by 0.2–3.1% compared with that of the control (soil pH of 8.01). Similar findings were also found in our study: after biochar was added to the coastal saline soil, the soil pH was slightly increased compared to that of the control (Table 1). This increase occurred because the pH of the wheat straw biochar was much higher than that of the soil (Table 1). Our study also found that biochar decreased the total salt content, and a similar result was reported by another researcher (Cui et al. 2022). This may be due to the fact that biochar decreased the soil salt content and water-soluble Na content of the soil profiles by improving the soil water content and adsorbing Na (Duan et al. 2021). The amendments enhanced SOM in our study, which may be due to the high carbon content of biochar (Gautam et al. 2021). In our study, the soil bulk density was significantly lower under the 79 t/hm² biochar treatment than under 0 t/hm² and 32 t/hm² biochar treatments. This was consistent with a previous study (Haeferle et al. 2011), which found that biochar application significantly reduced the soil bulk density. The reason for this decline was that the bulk density of the biochar was much lower than that of the soil (Table 1). Our experiment also found that the application of biochar (32, 79 t/hm²) significantly increased the soil MWD and macroaggregate (> 0.25 mm) content, which was consistent with previous findings (Fei et al. 2019; Liu et al. 2014). This may be due to the addition of biochar to the soil modified the bonding patterns of particles, thereby affecting the formation of macroaggregates (Yu et al. 2016). Brodowski et al. (2005) found that biochar usually did not exist in the form of dissociated organic matter in soil, but combined with the soil to form small soil masses or aggregates. In addition, some previous studies reported that adding PAM to soil enhanced the amount of soil macroaggregates and increased the stability of soil aggregates (Lentz 2015; Tang and She 2018). Our study also found that the soil

MWD and macroaggregate (>0.25 mm) content increased significantly with increasing PAM application. There were two reasons for this finding: one reason was the aggregation effect caused by PAM application; the other was that the application of PAM to the soil created a favorable soil environment for the growth of bacteria in soil aggregates (Caesar-TonThat et al. 2008).

Studies have shown that there is a close relationship between the photosynthetic rate and stomatal conductance ($P < 0.05$) (Attramadal et al. 1984). In our study, the change trend of the net photosynthetic rate was consistent with stomatal conductance after biochar application. These results are similar to the relationship between biochar and the gas exchange parameters of sugar beet found in a previous study (Zhang et al. 2020). Previous research by our research group showed that 32 t/hm² biochar treatment improved the soil pore structure (Sun et al. 2021). Soil total porosity can be improved by adding biochar (Oguntunde et al. 2008), and higher soil porosity provides a suitable growing environment for crop roots. Our experiment showed that the application of 32 t/hm² biochar could promote rice photosynthetic traits during the whole growth period but that the addition of excessive biochar (79 t/hm²) had no significant effect on photosynthetic traits. Similar results have been observed in previous studies (Feng et al. 2021; Ren et al. 2021). These results may be due to biochar with a high C/N ratio, which decreases crop nitrogen uptake and then reduces crop growth (Rajkovich et al. 2011). Moreover, amendments with a high C/N ratio can inhibit the absorption and utilization of light energy by photosynthetic system II (PSII) in rice leaves, leading to changes in the photosynthetic parameters of leaves; however, applying an appropriate amount of biochar may improve the light energy conversion efficiency, actual photosynthetic capacity, potential photosynthetic activity, and open PSII reaction center ratio in the leaves. In addition, biochar may enhance the capacity for the dissipation of excess light energy and decrease the inhibitory effect of environmental stress on photosynthesis, which may increase the stability of photosynthetic reaction centers and improve rice photosynthetic traits (Alimu et al. 2019; Saifullah Dahlawi et al. 2017).

Lentz (2015) observed that applying PAM to the soil increased the formation of soil water-stable aggregates, improved soil water conductivity, inhibited soil water evaporation, increased soil water retention, and thus improved the crop growth environment. Xu et al. (2016) found that soil amendment with PAM improved the leaf net photosynthetic rate, stomatal conductance, and transpiration rate of potato compared with the control, and similar results were observed in our experiment. Wei et al. (2011) found that different PAM treatments had no significant effect on the photosynthetic rate of maize, whereas the application of PAM decreased the transpiration rate compared with the control.

These findings are slightly different from the observed values in our experimental results.

Rice grain yield under biochar and PAM amendments

The application of biochar to soil does not always increase crop yields. Spokas et al. (2011) found that approximately 50% of published studies ($n = 45$) showed that biochar had positive effects on crop growth or yield, 30% of selected reports had no significant effect, and 20% even documented inhibited crop growth or yield. A 7-year field experiment showed that biochar application improved rice yield by enhancing the dynamics of root development and the characteristics of soil in Northwest China (Liu et al. 2020). Ali et al. (2020) reported that 60 t/hm² biochar addition coupled with 270 kg/hm² nitrogen fertilization had positive effects on the yield of noodle rice (Zhengui) using pot experiments in South China. Our experimental results showed that the 32 t/hm² biochar treatment caused an increase in grain yield relative to the control treatment but that the 79 t/hm² biochar treatment caused a decrease in grain yield, which was consistent with previous findings (Gaskin et al. 2010) showing that the grain yield of corn (*Zea mays* L.) first increased and then decreased with an increase in the application rate of peanut hull biochar (at 0, 11, and 22 Mg/ha) in fertilized treatments. This outcome may have been due to nitrogen mineralization; the soil nitrogen may have remained in the microbial biomass, preventing the nitrogen provided by the higher-rate biochar treatment from being used to support plant growth (Gaskin et al. 2010). Therefore, the application of biochar at an optimal level (e.g., 32 t/hm²) may enhance rice production in the selected soil, and the addition of more biochar (e.g., 76 t/hm²) should be carefully considered to avoid negative effects prior to application.

Lentz and Sojka (2009) found that two water-soluble anionic PAM treatments increased the yields of bean and silage corn by 14.3% and 4.5% in silt loam soils, respectively, and Wei et al. (2011) found that the addition of PAM at four rates (0.5, 1.0, 1.5, and 2.0 g/m²) improved maize yields by 5.54–14.13%. In our experimental results, the application of PAM (0.6, 1.6 t/hm²) increased the grain yield relative to that of the control, which was consistent with the results of previous studies (Lentz and Sojka 2009; Wei et al. 2011). The possible mechanism is that PAM treatment increased the lateral movement of water on the soil surface so that more water moved toward planted rows, creating a suitable environment for plant growth (Lentz et al. 1992). Our findings indicated that the rice grain yield was the highest under the combined application of 32 t/hm² biochar and 0.6 t/hm² PAM. This may have been due to the combined application of biochar and PAM directly or indirectly promoting soil water retention, increasing nutrient availability,

improving the physicochemical conditions of the saline soil, and thereby facilitating high agricultural productivity (Major et al. 2010; Lee et al. 2015).

The results from the path analysis showed that yield components had more significant positive direct effects on grain yield. In addition, grain yield was positively and significantly correlated with canopy gross photosynthesis, which is consistent with a previous study (Cheabu et al. 2018). This effect may have occurred because the CO₂ exchange rate in rice leaves increases linearly with an increase in the PAM application rate, and an increase in CO₂ exchange can increase photosynthesis (Lee et al. 2021). In addition, biochar and PAM may improve the leaf area of plants, and the leaf area makes a significant positive contribution to the photosynthetic rate (Wang et al. 2016a, b). Moreover, the level of total salt was significantly reduced by 32 t/hm² biochar application (Table 3), and the determination coefficient showed that soil total salt had a negative contribution to grain yield (Table 5). This indicated that biochar enhanced rice production by decreasing soil salinity (Cui et al. 2021).

In summary, our study showed the significant role of biochar and PAM in promoting the sustainability of rice production by revitalizing coastal saline soil and suggested a promising amelioration approach; this approach would restore agro-ecosystems and land resource sustainability and would have a far-reaching impact on food security. In addition, we found that the application of more amendments to the soil is not necessarily better, especially because large amounts of biochar (e.g., 79 t/hm²) may inhibit rice growth or yield. The application of amendments at an optimal level (e.g., 32 t/hm²) may increase rice growth or yield in coastal saline soil. An appropriate amount of amendments may play an important role in revitalizing soil quality and promoting sustainable land productivity.

Conclusions

- (1) The application of biochar and PAM improved saline soil properties. Biochar and PAM lowered the soil total salt and bulk density, but increased SOM, MWD, and macroaggregate (> 0.25 mm) content. The interaction of biochar and PAM had a significant effect on soil total salt.
- (2) The addition of biochar and PAM to saline soil had significant effects on the leaf photosynthetic traits of rice. The net photosynthetic rate and transpiration rate in the 32 t/hm² biochar and 1.6 t/hm² PAM treatments were significantly higher than those in the control; moreover, the effect of the combined application of 32 t/hm² biochar + 0.6 t/hm² PAM on the net photosynthetic rate and transpiration rate was the most significant.
- (3) The appropriate addition of biochar and PAM to saline soil increased rice grain yield. Spikelets per panicle and

canopy gross photosynthesis had strong and significant positive effects on grain yield. Biochar enhanced the rice grain yield by decreasing the soil salinity.

Supplementary Information The online version contains supplementary material available at <https://doi.org/10.1007/s11356-022-23511-w>.

Author contribution AA contributed to the conception of the research article; AA conducted the data analysis and interpretation of the results of the paper, and wrote and organized the manuscript; DS contributed to the refinement of the article conception and experimental design and to the logical structure of the manuscript; ZL contributed to data analysis and manuscript preparation; XS and HW performed the data analysis as well as the interpretation of the results.

Funding This research article was financially supported by the National Natural Science Foundation of China (42177393), the Water Science and Technology Project of Jiangsu Province (grant number 2021054), the Natural Resources Science and Technology Project of Jiangsu Province (grant number 2022046), and Study on Optimal Allocation of Agricultural Water and Soil Resources in Coastal Areas (2022005).

Data availability The datasets analyzed during the current study are available from the corresponding author on reasonable request.

Declarations

Ethics approval Not applicable.

Consent to participate Not applicable.

Consent for publication Not applicable.

Competing interests The authors declare no competing interests.

References

- Ajayi AE, Holthusen D, Horn R (2016) Changes in microstructural behaviour and hydraulic functions of biochar amended soils. *Soil Tillage Res* 155:166–175
- Ali S, Rizwan M, Qayyum MF, Ok YS (2017) Biochar soil amendment on alleviation of drought and salt stress in plants: a critical review. *Environ Sci Pollut Res* 24:12700–12712
- Alimu A, Yao H, Song Y, Fei Y, She D (2019) Effects of soil structure improvement on chlorophyll fluorescence parameters and yield of rice in a coastal reclamation region. *Chin J Appl Ecol* 30(10):3435–3442 (in Chinese)
- Ali I, He L, Ullah S, Quan Z (2020) Biochar addition coupled with nitrogen fertilization impacts on soil quality, crop productivity, and nitrogen uptake under double-cropping system. *Food Energy Secur* 9:1–20
- Attramadal H, Jahnsen T, Hansson V (1984) Regulation of hormone-responsive Sertoli cell adenylyl cyclase in a cell-free system. *Mol Cell Endocrinol* 34:221–228
- Brodowski S, Amelung W, Haumaier L, Abetz C, Zech W (2005) Morphological and chemical properties of black carbon in physical soil fractions as revealed by scanning electron microscopy and energy-dispersive X-ray spectroscopy. *Geoderma* 128(1–2):116–129
- Caesar-TonThat TC, Busscher WJ, Novak JM, Gaskin JF, Kim Y (2008) Effects of polyacrylamide and organic matter on microbes

- associated to soil aggregation of Norfolk loamy sand. *Appl Soil Ecol* 40(2):240–249
- Cheabu S, Mounq-Ngam P, Arikat S (2018) Effects of heat stress at vegetative and reproductive stages on spikelet fertility. *Rice Sci* 25:218–226
- Cueff S, Coquet Y, Aubertot JN, Bel L, Pot V, Alletto L (2021) Estimation of soil water retention in conservation agriculture using published and new pedotransfer functions. *Soil Tillage Res* 209:104967
- Cui L, Liu Y, Yan J, Hina K, Hussain Q, Qiu T, Zhu J (2022) Revitalizing coastal saline-alkali soil with biochar application for improved crop growth. *Ecol Eng* 179:106594
- Cui Q, Xia J, Yang H, Liu J, Shao P (2021) Biochar and effective microorganisms promote *Sesbania cannabina* growth and soil quality in the coastal saline-alkali soil of the Yellow River Delta. *China Sci Total Environ* 756:143801
- Ding JL, Yu DL (2014) Monitoring and evaluating spatial variability of soil salinity in dry and wet seasons in the Werigan-Kuqa Oasis, China, using remote sensing and electromagnetic induction instruments. *Geoderma* 235–236:316–322
- Duan M, Liu G, Zhou B, Chen X, Wang Q, Zhu H, Li Z (2021) Effects of modified biochar on water and salt distribution and water-stable macro-aggregates in saline-alkaline soil. *J Soils Sediments* 21(6):2192–2202
- Fei YH, She DL, Gao L (2019) Micro-CT assessment on the soil structure and hydraulic characteristics of saline/sodic soils subjected to short-term amendment. *Soil Tillage Res* 193:59–70
- Feng WY, Yang F, Cen R (2021) Effects of straw biochar application on soil temperature, available nitrogen and growth of corn. *J Environ Manage* 277:111331
- Gaskin JW, Speir RA, Harris K (2010) Effect of peanut hull and pine chip biochar on soil nutrients, corn nutrient status, and yield. *Agron J* 102:623–633
- Gautam RK, Goswami M, Mishra RK, Chaturvedi P, Awashthi MK, Singh RS, Giri BS, Pandey A (2021) Biochar for remediation of agrochemicals and synthetic organic dyes from environmental samples: A review. *Chemosphere* 272:129917
- Guner OI, Goktas A, Kayali U (2017) Path analysis and determining the distribution of indirect effects via simulation. *J Appl Stat* 44:1181–1210
- Haefele SM, Konboon Y, Wongboon W, Amarante S, Maarifat AA, Pfeiffer EM, Knoblauch C (2011) Effects and fate of biochar from rice residues in rice-based systems. *Field Crops Res* 121(3):430–440
- Han FP, Zheng JY, Li ZB (2010) Effect of PAM on soil physical properties and water distribution. *Transactions of the CSAE* 26:70–74 (in Chinese)
- Hardie M, Clothier B, Bound S, Oliver G, Close D (2014) Does biochar influence soil physical properties and soil water availability? *Plant Soil* 376(1–2):347–361
- Lee HJ, Lee JH, Wi S (2021) Exogenously applied glutamic acid confers improved yield through increased photosynthesis efficiency and antioxidant defense system under chilling stress condition in *Solanum lycopersicum* L. cv. Dotaerang. *Dia Sci Hort* 277:1–9
- Lee SS, Shah HS, Awad YM (2015) Synergy effects of biochar and polyacrylamide on plants growth and soil erosion control. *Environ Earth Sci* 74:2463–2473
- Lentz RD (2003) Inhibiting water infiltration with polyacrylamide and surfactants: applications for irrigated agriculture. *J Soil Water Conserv* 58:290–300
- Lentz RD (2015) Polyacrylamide and biopolymer effects on flocculation, aggregate stability, and water seepage in a silt loam. *Geoderma* 241–242:289–294
- Lentz RD, Shainberg I, Sojka RE (1992) Preventing irrigation furrow erosion with small applications of polymers. *Soil Sci Soc Am J* 56:1926–1932
- Lentz RD, Sojka RE (2009) Long-term polyacrylamide formulation effects on soil erosion, water infiltration, and yields of furrow-irrigated crops. *Agron J* 101:305–314
- Liu BT, Li HL, Li HB (2020) Long-term biochar application promotes rice productivity by regulating root dynamic development and reducing nitrogen leaching. *GCB Bioenergy* 13:257–268
- Liu X, Liu C, Gao W, Xue C, Guo Z, Jiang L, Li F, Liu Y (2019) Impact of biochar amendment on the abundance and structure of diazotrophic community in an alkaline soil. *Sci Total Environ* 688:944–951
- Liu Z, Chen X, Jing Y, Li Q, Zhang J, Huang Q (2014) Effects of biochar amendment on rapeseed and sweet potato yields and water stable aggregate in upland red soil. *CATENA* 123:45–51
- Major J, Rondon M, Molina D (2010) Maize yield and nutrition during 4 years after biochar application to a Colombian savanna oxisol. *Plant Soil* 333:117–128
- Miao ZM, Yu SE, Lu B (2013) Relationships of ‘water requirement-photosynthesis-production’ for paddy rice using structural equation modeling. *Transactions of the CSAE* 29:91–98 (in Chinese)
- Nadler A, Perfect E, Kay BD (1996) Effect of polyacrylamide application on the stability of dry and wet aggregates. *Soil Sci Soc Am J* 60:555–561
- O’Laughlin J, McElligott K (2009) Biochar for environmental management: science and technology. *Forest Policy Econ* 11:535–536
- Oguntunde PG, Abiodun BJ, Ajayi AE (2008) Effects of charcoal production on soil physical properties in Ghana. *J Plant Nutr Soil Sci* 171:591–596
- Pury D, Farquhar GD (1997) Simple scaling of photosynthesis from leaves to canopies without the errors of big-leaf models. *Plant Cell Environ* 20:537–557
- Rajkovich S, Enders A, Hanley K, Hyland C, Zimmerman AR, Lehmann J (2011) Corn growth and nitrogen nutrition after additions of biochars with varying properties to a temperate soil. *Biol Fertil Soils* 48(3):271–284
- Ren TB, Chen N, Wan Mahari WA (2021) Biochar for cadmium pollution mitigation and stress resistance in tobacco growth. *Environ Res* 192:110273
- SaifullahDahlawi S, Naeem A, Rengel Z, Naidu R (2017) Biochar application for the remediation of salt-affected soils: challenges and opportunities. *Sci Total Environ* 625:320–335
- Schepetkin IA, Khlebnikov AI, Ah SY (2003) Characterization and biological activities of humic substances from mumie. *J Agric Food Chem* 51:5245–5254
- Sohi SP, Krull E, Lopez-Capel E (2010) A review of biochar and its use and function in soil. *Adv Agron* 105:47–82
- Spokas KA, Cantrell KB, Novak JM, Archer DW, Ippolito JA, Collins HP, Boateng AA, Lima IM, Lamb MC, McAloon AJ, Lentz RD, Nichols KA (2011) Biochar: a synthesis of its agronomic impact beyond carbon sequestration. *J Environ Qual* 41(4):973–989
- Sun XQ, She DL, Fei YH (2021) Three-dimensional fractal characteristics of soil pore structure and their relationships with hydraulic parameters in biochar-amended saline soil. *Soil Tillage Res* 205:1–12
- Tang SQ, She DL (2018) Synergistic effects of rock fragment cover and polyacrylamide application on erosion of saline-sodic soils. *CATENA* 171:154–165
- Tatum M (2021) China’s three-child policy. *Lancet* 397:2238
- Tejada M, Gonzalez JL (2007) Influence of organic amendments on soil structure and soil loss under simulated rain. *Soil Tillage Res* 93:197–205
- Wang MH, Li M, Gao Q (2016a) Effects of amendments on growth and physiological characteristics of maize seedlings on saline-alkali soil. *Chinese J Eco* 35:2966–2973 (in Chinese)
- Wang WG, Ding YM, Shao QX (2017) Bayesian multi-model projection of irrigation requirement and water use efficiency in three typical rice plantation region of China based on CMIP5. *Agric for Meteorol* 232:89–105

- Wang Y, Zhang JH, Zhang ZH (2015) Influences of intensive tillage on water-stable aggregate distribution on a steep hillslope. *Soil Tillage Res* 151:82–92
- Wang YQ, Xi WX, Wang ZM (2016b) Contribution of ear photosynthesis to grain yield under rainfed and irrigation conditions for winter wheat cultivars released in the past 30 years in North China Plain. *J Integr Agr* 15:2247–2256
- Wei XD, Yuan XF, Li YM (2011) Research on the water-saving and yield-increasing effect of polyacrylamide. *Procedia Environ Sci* 11:573–580
- Xu CY, Hosseini-Bai S, Hao Y, Rachaputi RC, Wang H, Xu Z, Wallace H (2015) Effect of biochar amendment on yield and photosynthesis of peanut on two types of soils. *Environ Sci Pollut Res* 22(8):6112–6125
- Xu ST, Lei Z, McLaughlin NB (2016) Effect of synthetic and natural water-absorbing soil amendments on photosynthesis characteristics and tuber nutritional quality of potato in a semi-arid region. *J Sci Food Agr* 96:1010–1017
- Xu Y, Pu LJ, Liao QL (2017) Spatial variation of soil organic carbon and total nitrogen in the coastal area of mid-eastern China. *Int J Environ Res Pub Heal* 14:780
- Yang JS (2008) Improvement of salt-affected soils in China. *Acta Pedol Sin* 45:837–845 (in Chinese)
- Yu HY, Zha TG, Zhang XX (2019) Vertical distribution and influencing factors of soil organic carbon in the Loess Plateau, China. *Sci Total Environ* 693:133632.1–133632.8
- Yu J, Wu LT, Shainberg I (2010) Effects of different application methods of polyacrylamide (PAM) on soil infiltration and erosion. *Transactions of the CSAE* 26:38–44 (in Chinese)
- Yu X, Wu C, Fu Y, Brookes PC, Lu S (2016) Three-dimensional pore structure and carbon distribution of macroaggregates in biochar-amended soil. *Eur J Soil Sci* 67(1):109–120
- Zhao W, Zhou Q, Tian Z, Cui Y, Liang Y, Wang H (2020) Apply biochar to ameliorate soda saline-alkali land, improve soil function and increase corn nutrient availability in the Songnen Plain. *Sci Total Environ* 722:137428
- Zhang PF, Yang FF, Zhang H (2020) Beneficial effects of biochar-based organic fertilizer on nitrogen assimilation, antioxidant capacities, and photosynthesis of sugar beet (*Beta vulgaris* L.) under saline-alkaline stress. *Agronomy* 10:1562
- Zhou H, Fang H, Zhang Q, Wang Q, Chen C, Mooney SJ, Peng X, Du Z (2018) Biochar enhances soil hydraulic function but not soil aggregation in a sandy loam. *Eur J Soil Sci* 70(2):291–300

Publisher's note Springer Nature remains neutral with regard to jurisdictional claims in published maps and institutional affiliations.

Springer Nature or its licensor holds exclusive rights to this article under a publishing agreement with the author(s) or other rightsholder(s); author self-archiving of the accepted manuscript version of this article is solely governed by the terms of such publishing agreement and applicable law.